Optimal Differentiator Filter Banks for PMUs and their Feasibility Limits

Francisco Messina, Leonardo Rey Vega, Pablo Marchi, Cecilia G. Galarza

***Abstract*—In this paper, we present a very general design approach for optimal linear-phase phasor filter bank algorithms for PMUs based on convex semi-infinite optimization. A detailed presentation of the formulation of both the cost functions and constraints is included for the positive-sequence estimation problem. The design method is extremely powerful and flexible as it allows to control precisely the behavior of the system in terms of the total vector error (TVE), frequency error (FE), and rate of change of frequency error (RFE) metrics for several different scenarios. This feature is extremely useful for tailored designs of these filters for different applications. We also determine numerically the uniform feasibility limits of the system as a function of the filter lengths and, in particular, study the required filter lengths for compliance with the IEEE Standards C37.118.1-2011 and C37.118.1a-2014. It is found that all requirements can be achieved with a significant margin with the exception of the M class FE constraint for interharmonic components, an issue which is also reported in other works and briefly discussed here. Finally, an interesting comparison with the Taylor-Fourier filters is made to illustrate the advantages of our approach.**

I. Introduction

A. Review and Motivation

Phasor Measurement Units (PMUs) are at the core of wide-area measurement systems (WAMS), which provide timely situational awareness to modern power systems. These devices produce fast and accurate measurements of phasor, frequency and rate of change of frequency (ROCOF) of voltage and current power signals. This is possible because PMUs are synchronized with the UTC global time standard, usually by means of a GPS receiver. The IEEE Std. C37.118.1-2011 [1] on synchrophasors and its recent amendment C37.118.1a-2014 [2] establish precise and strict requirements on these measurements. They are classified as stationary and dynamic requirements but can alternatively be divided into time and frequency domain constraints.

A considerable amount of research was conducted in synchrophasor estimation algorithms, particularly in the last decade. Originally, phasor estimation was performed with a DFT, which is both efficient and provides perfect rejection of harmonics at nominal frequency [3]. Several improvements of the algorithm were proposed to improve the behavior in off-nominal conditions where leakage effects appear [4], [5]. However, the method is inherently limited in dynamic conditions because it is based on a stationary model. An important contribution was the recognition of the importance of the dynamic phasor concept in power systems [6], showing the limitations of the steady-state phasor model for synchrophasor estimations. This led to the Taylor-Fourier (TF) filters, which are given by the LS [6] or WLS [7] solutions to the Taylor approximation of the dynamic phasor as well as several other methods such as the IpD^{2}FT [8]. A detailed comparison of some of the previous algorithms can be found in [9], [10]. The dynamic model is much more accurate than a stationary one, but it has at least two important limitations. First, interference components such as harmonics and interharmonics are not explicitly taken into account. In fact, they are treated as noise without a precise mathematical structure. Thus, poor performance is obtained when these disturbances are present [11]. Although it is possible to extend the model to include the estimation of these components to improve the one of the fundamental phasor [12], this requires prior knowledge of the interharmonic frequency components and considerably increases the computational cost of the algorithm. Secondly, it is limited by the assumed parametric polynomial model which, for example, is not convenient for discontinuities in the dynamic phasor such as the ones that are present when a sudden change in amplitude or phase occurs. On the other hand, filter design criteria for synchrophasor estimation were studied lately based on frequency domain constraints [13], [14], which yielded spectral masks for magnitude response requirements. However, the main limitation of these criteria is that they do not take into account, in precise terms, the relevant time domain constraints, which means that not all of the IEEE Std. requirements are incorporated into the design and therefore the problem formulation is incomplete.

Most of the aforementioned methods have a common feature: they generally need some degree of parameter tuning to work properly for a particular set of requirements. Moreover, it is not always well-known how to control the performance of the method for a given signal waveform, nor if it is feasible to achieve a set of requirements before an exhaustive set of tests is performed. This is clearly a disadvantage for the designer, since it leads to a time-consuming trial and error process.

B. Contribution and Challenges

The contribution of this work is to present thoroughly a general and flexible approach for designing optimal filter bank systems for dynamic phasor estimation. It is based on convex

The work of F. Messina was supported by a Peruilh Ph.D. grant from Universidad de Buenos Aires. This work was partially funded by the UREE 4 FONARSEC project: "Development of Synchrophasor Measurements for Smart Electrical Grids". The FONARSEC is funded by the Ministry of Science, Technology and Innovaton of Argentina.

F. Messina, L. Rey Vega, P. Marchi, and C. G. Galarza are with the CSC-CONICET, and the School of Engineering - Universidad de Buenos Aires, Argentina (e-mail: fmessina@fi.uba.ar, lrey@fi.uba.ar, pmarchi@fi.uba.ar, cgalar@fi.uba.ar).

semi-infinite programming (CSIP), a powerful tool for optimal digital filter design [15], [16], [17]. Basically, it extends the idea of the work [18] to a filter bank (FB) which provides not only a phasor estimate but also phasor derivative estimates. As it will be shown, this approach provides total control of the FB performance at the design stage in both time and frequency domains.

There are several challenges that were encountered to complete this work. The major one is recognizing the fact that the synchrophasor estimation problem can be posed as three convex semi-infinite optimization programs. This is not a trivial observation. In fact, as can be seen in Section II, it requires a very careful formulation of the whole problem. To the best of our knowledge, this is the first time that the synchrophasor estimation problem is posed explicitly and completely (with all time and frequency domain constraints) as an optimization problem. As minor challenges, but still important to obtain useful numerical results, we can mention the following:

1) The simplification of the constraints to obtain a problem that is computationally simpler and suitable for the available solvers.
2) Performing the feasibility analysis of the problem.

C. Organization

The rest of the paper is organized as follows. In Section II, the FB is introduced and then the filter optimization problem for the design of this system is formulated as a convex semi-infinite program. The limits of this structure are then analyzed with computer simulations in Section III, and case studies for both P and M class PMUs are presented to show the features of the filters obtained with this approach. Finally, conclusions and comments about future research directions are given in Section IV.

II. Filter Bank Design

A. Motivation

The filter bank estimation system is presented in Fig. 1, where $\mathcal{X}[n]$ is the signal phasor, $\mathcal{I}[n]$ is a nuisance phasor, $\mathcal{Y}[n]$ is the input phasor to the system, $\widehat{\mathcal{X}}[n]$ is the phasor estimate, $\widehat{\mathcal{X}'}[n]$ is the first derivative phasor estimate, and $\widehat{\mathcal{X}''}[n]$ is the second derivative phasor estimate. The sampling period is denoted by T and all phasors are assumed to be baseband signals. Note that $\mathcal{I}[n]$ may represent an actual interference signal, unbalances for a three-phase signal, a double-frequency image component for a single-phase signal, or simply random noise. Each case can be treated by an appropriate constraint, illustrating the generality of this approach. The blocks $A_i(\nu)$, $i = 0, 1, 2$, represent zero-phase finite impulse response (FIR) filters, that is, systems which produce no delay. In practice, they arise from linear-phase filters $H_i(\nu)$ and the required system latency to compensate for the delay that they cause. This is equivalent to centering the filter window around each report time, a popular strategy in synchrophasor estimation algorithms. In [18], the filter A_0 is presented as a general dynamic phasor estimator and motivated for both single- and three-phase synchrophasor estimation systems. This is a natural extension for the case where the first- and second-order phasor derivatives are also required. Given the estimates $\widehat{\mathcal{X}}[n]$, $\widehat{\mathcal{X}'}[n]$, and $\widehat{\mathcal{X}''}[n]$, it is a simple matter to obtain $\widehat{\omega}[n]$, and $\widehat{\alpha}[n]$, that is, the angular frequency and angular rate of change of frequency (ROCOF) estimates, with the following relations:

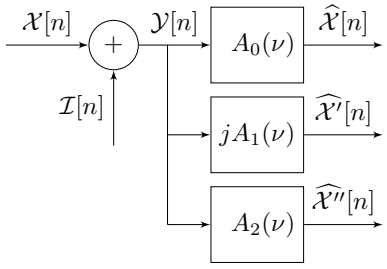

Fig. 1. General zero-phase filter bank system.

$$\widehat{\omega}[n] = \operatorname{Im}\left\{\frac{\widehat{\mathcal{X}'}[n]}{\widehat{\mathcal{X}}[n]}\right\},$$
$$\widehat{\alpha}[n] = \operatorname{Im}\left\{\frac{\widehat{\mathcal{X}''}[n]}{\widehat{\mathcal{X}}[n]}\right\} - 2\operatorname{Re}\left\{\frac{\widehat{\mathcal{X}'}[n]}{\widehat{\mathcal{X}}[n]}\right\}\operatorname{Im}\left\{\frac{\widehat{\mathcal{X}'}[n]}{\widehat{\mathcal{X}}[n]}\right\}. \quad (1)$$

These expressions are similar to those that appear in [8] and were introduced, in a slightly different manner, in [6]. They will be used extensively in what follows to obtain the design constraints for the filter bank design problem.

In this section, it will be shown that the filter bank design problem can be posed in the framework of convex semi-infinite programming, whose solution can then be found by any of the several available solvers [19], [20]. Due to space constraints, only the problem of estimating the positive-sequence phasor and its derivatives will be treated but, as mentioned above, it should be clear that the approach is not limited to this problem. We will focus mainly on the IEEE Std. requirements but will also show how to include other constraints for tailored designs.

B. Definitions

The first filter $A_0(\nu)$, which estimates the signal phasor, is chosen as a type I FIR filter as in [18] to produce an even amplitude response filter with integer group delay. Similarly, the second filter $jA_1(\nu)$, which is a first-order differentiator filter, is chosen as a type III filter to produce an odd amplitude response filter with integer group delay. Finally, the third filter $A_2(\nu)$, which is a second-order differentiator filter, is again a type I filter. The filter orders are considered to be equal without loss of generality and are denoted by N. Then, the expressions for the amplitude responses are as follows:

$$A_i(\nu) = \mathbf{g}_i^T(\nu)\,\mathbf{a}_i, \qquad i = 0, 1, 2,$$

where $\mathbf{g}_0(\nu) = [1, \cos(\nu), \ldots, \cos(R\nu)]^T$, $\mathbf{g}_1(\nu) = [\sin(\nu), \ldots, \sin(R\nu)]^T$, $\mathbf{g}_2(\nu) = \mathbf{g}_0(\nu)$, and $R = N/2$. The vectors $\mathbf{a}_i$ represent the linear-phase representation filter coefficients.

C. Cost Functions

The choice of the cost functions for the optimization problems is by no means unique and may depend on the particular application of the synchrophasor measurements. Here, we propose to define the cost functions on the basis of a uniform bound of the squared error criterion as in [18] but generalized to account also for interference perturbations:

$$f_i(\mathbf{a}_i) = \lambda_i \left\| A_i - A_i^{\mathrm{id}} \right\|_{2,\Omega_1}^2 + (1-\lambda_i) \left\| A_i \right\|_{2,\Omega_2}^2, \quad (2)$$

with $i = 0, 1, 2$, and where Ω_1 is the union of the passband and transition band of the filters, while Ω_2 is the stopband. They are defined according to the IEEE Std. specifications. Functions A_i^{id} are the ideal responses of each filter in the passband: $A_0^{\mathrm{id}}(\nu) = 1$, $A_1^{\mathrm{id}}(\nu) = \frac{\nu}{T}$, and $A_2^{\mathrm{id}}(\nu) = -\frac{\nu^2}{T^2}$. Also, $\lambda_i \in [0,1]$ are defined according to the desired trade-off between phasor signal distortion and interference power reduction. Note that the objective functions f_i are quadratic functions of $\mathbf{a}_i$ and can be written as $f_i(\mathbf{a}_i) = \mathbf{a}_i^T \boldsymbol{P}_i \mathbf{a}_i + \mathbf{q}_i^T \mathbf{a}_i + r_i$, where $\boldsymbol{P}_i, \mathbf{q}_i$ and r_i are readily found from (2). Since $\boldsymbol{P}_i$ are positive semi-definite matrices, it follows that f_i are convex functions.

D. Optimization problem

For each of the desired filters ($i = 0, 1, 2$), the optimization problem $\mathcal{P}_i$ can be cast as:

$$\mathcal{P}_i : \min_{\mathbf{a}_i} f_i(\mathbf{a}_i)$$
$$\text{s.t. } h_{ik}(\mathbf{a}_i, \nu_{ik}, \theta_{ik}) \le c_{ik},$$

where $(\nu_{ik}, \theta_{ik}) \in \Omega_{ik} \times \Theta_{ik}, k = 1, \ldots, M_i$, h_{ik} are appropriate convex functions in $\mathbf{a}_i$ that summarize the several time and frequency domain constraints to be achieved by the i-th filter, and c_{ik} are desired performance levels. Note that some of these functions[1] can depend on a frequency variable ν_{ik} and other continuous parameter θ_{ik} particular to that specific requirement. As Ω_{ik} and Θ_{ik} can be infinite sets (such as closed intervals), it is said that these constraints are semi-infinite ones. In this way, the above problem can be recognized as one of convex semi-infinite programming, a very well developed field of optimization [16]. The solution approach we take is as follows. First we solve the problem $\mathcal{P}_0$, which yields the filter A_0^* (determined by $\mathbf{a}_0^*$). Then, the problem $\mathcal{P}_1$ is formulated which, as will be shown below, depends on the optimal $\mathbf{a}_0^*$ already obtained. Similarly, for the problem $\mathcal{P}_2$, the constraints depend on $\mathbf{a}_0^*$ and $\mathbf{a}_1^*$. This induces a sequential procedure for solving the problem. Clearly, our solution approach for obtaining the desired filters is suboptimal, but has the important advantage of producing a sequence of convex subproblems, thus guaranteeing that a global optimum can be found for each individual optimization problem. It remains to obtain the corresponding expressions for the functions h_{ik} and the desired levels of performance c_{ik}. This is done in the following subsections.

[1]The formulation also allows to incorporate ordinary convex constraints by letting some of the functions h_{ik} to be constant with respect to the semi-infinite parameters.

E. Off-Nominal Signal Frequency Constraints

In this case, the input phasor is $\mathcal{Y}[n] = \mathcal{X}[n] = a_s e^{j(\nu_s n + \phi_s)}$, where ν_s is the phasor angular frequency with respect to the nominal frequency, which belongs to a given set Ω_s. If we force the steady-state TVE to be below some upper bound $\mathrm{TVE}_{\mathrm{STA}}$, we obtain the following convex semi-infinite constraint:

$$\mathrm{TVE} = |A_0(\nu_s) - 1| \le \mathrm{TVE}_{\mathrm{STA}}, \qquad \nu_s \in \Omega_s.$$

Similarly, evaluating FE with the expressions in (1), and using an upper limit $\mathrm{FE}_{\mathrm{STA}}$, we obtain:

$$\mathrm{FE} = \frac{1}{2\pi} \left| \frac{A_1(\nu_s)}{A_0^*(\nu_s)} - \frac{\nu_s}{T} \right| \le \mathrm{FE}_{\mathrm{STA}}, \qquad \nu_s \in \Omega_s.$$

It is easy to see from (1) that for the signal model assumed RFE is exactly zero due to the fact that the filters A_i are real. This implies that there is not a constraint associated with A_2.

F. Interference Rejection Constraints

When an interference is present, the input phasor is $\mathcal{Y}[n] = \mathcal{X}[n] + \mathcal{I}[n] = a_s e^{j(\nu_s n + \phi_s)} + a_i e^{j(\nu_i n + \phi_i)}$, where ν_i is the interference phasor angular frequency which belongs to a given set Ω_i. Forcing the worst-case steady-state TVE to be below an upper bound $\mathrm{TVE}_{\mathrm{INT}}$, we get:

$$|A_0(\nu_s) - 1| + |A_0(\nu_i)|\eta \le \mathrm{TVE}_{\mathrm{INT}}, \qquad (\nu_s, \nu_i) \in \Omega_s \times \Omega_i,$$

where $\eta = a_i/a_s$. To find the constraint that ensures that FE is smaller than a desired limit $\mathrm{FE}_{\mathrm{INT}}$, we first express the frequency estimation in (3), at the bottom of the next page, where $\theta = (\nu_i - \nu_s)n + (\phi_i - \phi_s)$. Thus, the FE constraint is

$$\left| \widehat{\omega}(\nu_s, \nu_i, \theta) - \frac{\nu_s}{T} \right| \le 2\pi \mathrm{FE}_{\mathrm{INT}}, \ (\nu_s, \nu_i, \theta) \in \Omega_s \times \Omega_i \times [-\pi, \pi].$$

However, for computational purposes, it is desirable to simplify this three-parameter semi-infinite constraint into one or more two-parameter semi-infinite constraints. Since maximum and minimum values for the estimated frequency occur[2] when $\theta = 0$ or $\theta = \pi$, the FE constraint may be expressed as two semi-infinite constraints in two semi-infinite parameters:

$$\left| \widehat{\omega}(\nu_s, \nu_i, 0) - \frac{\nu_s}{T} \right| \le 2\pi \mathrm{FE}_{\mathrm{INT}}, \qquad (\nu_s, \nu_i) \in \Omega_s \times \Omega_i,$$
$$\left| \widehat{\omega}(\nu_s, \nu_i, \pi) - \frac{\nu_s}{T} \right| \le 2\pi \mathrm{FE}_{\mathrm{INT}}, \qquad (\nu_s, \nu_i) \in \Omega_s \times \Omega_i.$$

Finally, the RFE constraint is formally as follows:

$$|\widehat{\alpha}(\nu_s, \nu_i, \theta)| \le 2\pi \mathrm{RFE}_{\mathrm{INT}}, \qquad (\nu_s, \nu_i, \theta) \in \Omega_s \times \Omega_i \times [-\pi, \pi], \quad (4)$$

where the expression of $\widehat{\alpha}(\nu_s, \nu_i, \theta)$ is given in (5), again at the bottom of the next page. Unfortunately, there is not a simple equivalent two-parameter constraint for this case, so we will seek for an approximation. In order to do so, note from (5) that if we neglect the second term for one moment[3], and note that $2A_0^*(\nu_i)\eta \ll A_0^*(\nu_s)$, we obtain an

[2]A function of the form $f(\theta) = (x + y\cos\theta)/(w + z\cos\theta)$ which is well defined for all $\theta \in [-\pi, \pi]$ has stationary points at $\theta = \pm\pi$, and $\theta = 0$. Thus, its maximum and minimum values are either $f(0)$ or $f(\pi)$.

[3]This is justified since the stopband ripples of A_0 and A_1 are generally much smaller than those of A_2.

approximation of $\widehat{\alpha}(\nu_s,\nu_i,\theta)$ that is sinusoidal in θ. Under this approximation, $|\widehat{\alpha}(\nu_s,\nu_i,\theta)|$ is maximum for $\theta=\pm\pi/2$. Therefore, we propose the following relaxation of (4):

$$|\widehat{\alpha}(\nu_s,\nu_i,-\pi/2)|\le 2\pi\text{RFE}_{\text{INT}}, \qquad (\nu_s,\nu_i)\in\Omega_s\times\Omega_i,$$
$$|\widehat{\alpha}(\nu_s,\nu_i,+\pi/2)|\le 2\pi\text{RFE}_{\text{INT}}, \qquad (\nu_s,\nu_i)\in\Omega_s\times\Omega_i.$$

G. Amplitude and Phase Modulation Constraints

The signal phasor for an amplitude modulated signal is $\mathcal{X}[n]=a_s[1+k_a\cos(\nu_m n+\phi_m)]e^{j\phi_s}$. Evaluating the TVE and forcing the condition $\text{TVE}[n]\le\text{TVE}_{\text{AM}}$ for all $n\in\mathbb{Z}$, we obtain the following constraints:

$$\frac{|(A_0(0)-1)+(A_0(\nu_m)-1)k_a|}{|1+k_a|}\le\text{TVE}_{\text{AM}}, \qquad \nu_m\in\Omega_m,$$
$$\frac{|(A_0(0)-1)-(A_0(\nu_m)-1)k_a|}{|1-k_a|}\le\text{TVE}_{\text{AM}}, \qquad \nu_m\in\Omega_m,$$

where Ω_m is the set of possible modulation frequencies. Generally, these constraints are implied by the TVE off-nominal frequency constraint. Nevertheless, for the sake of generality, we shall keep the constraint in the formulation. On the other hand, since $A_1(0)=0$ for all $\mathbf{a}_1$, both FE and RFE are exactly zero, so that no additional constraints are required.

For the phase modulation signal, the input phasor is [21]: $\mathcal{X}[n]=a_s e^{j\phi_s}e^{jk_\phi\cos(\nu_m n+\phi_m)}=a_s e^{j\phi_s}\left(\mathcal{X}_R[n]+j\mathcal{X}_I[n]\right)$, where $\mathcal{X}_R[n]=J_0(k_\phi)+2\sum_{k=1}^{\infty}(-1)^k J_{2k}(k_\phi)\cos(2k\theta_m)$, $\mathcal{X}_I[n]=2\sum_{k=0}^{\infty}(-1)^k J_{2k+1}(k_\phi)\cos[(2k+1)\theta_m]$, $\theta_m=\nu_m n+\phi_m$, and J_k is the k-th order Bessel function of the first kind. Note that $J_k(k_\phi)$ rapidly decays to zero[4] as $k\to\infty$ for typical values of the modulation factor k_ϕ. Therefore, a few terms are often sufficient to approximate the input phasor. The filter bank outputs are given by: $\widehat{\mathcal{X}}[n]=a_s e^{j\phi_s}(\widehat{\mathcal{X}_R}[n]+j\widehat{\mathcal{X}_I}[n])$, $\widehat{\mathcal{X}'}[n]=a_s e^{j\phi_s}(\widehat{\mathcal{X}'_R}[n]+j\widehat{\mathcal{X}'_I}[n])$, $\widehat{\mathcal{X}''}[n]=a_s e^{j\phi_s}(\widehat{\mathcal{X}''_R}[n]+j\widehat{\mathcal{X}''_I}[n])$, where $\widehat{\mathcal{X}_R}[n]$, $\widehat{\mathcal{X}_I}[n]$, $\widehat{\mathcal{X}'_R}[n]$, $\widehat{\mathcal{X}'_I}[n]$, $\widehat{\mathcal{X}''_R}[n]$, and $\widehat{\mathcal{X}''_I}[n]$ are defined in (6) at the bottom of the next page. For simplicity, we work with the squared TVE, which is a convex quadratic function of $\mathbf{a}_0$ and depends on the semi-infinite parameters ν_m and θ_m. Therefore, we obtain the following convex semi-infinite constraint:

$$\text{TVE}^2(\nu_m,\theta_m)\le\text{TVE}^2_{\text{PM}}, \qquad (\nu_m,\theta_m)\in\Omega_m\times[-\pi,\pi],$$

The FE constraint is as follows:

$$\left|\widehat{\omega}(\nu_m,\theta_m)+\frac{k_\phi\nu_m}{T}\sin(\theta_m)\right|\le 2\pi\text{FE}_{\text{PM}},$$

for all $(\nu_m,\theta_m)\in\Omega_m\times[-\pi,\pi]$, where $\widehat{\omega}(\nu_m,\theta_m)$ is the frequency estimate, which is a real linear function of $\mathbf{a}_1$. Similarly, the RFE constraint is.

$$\left|\widehat{\alpha}(\nu_m,\theta_m)+\frac{k_\phi\nu_m^2}{T^2}\cos(\theta_m)\right|\le 2\pi\text{RFE}_{\text{PM}},$$

for all $(\nu_m,\theta_m)\in\Omega_m\times[-\pi,\pi]$, where $\widehat{\alpha}(\nu_m,\theta_m)$ is a real affine function of $\mathbf{a}_2$.

[4]Formally, we have the following asymptotic result [21]:

$$J_\alpha(x)=\frac{1}{\Gamma(\alpha+1)}\left(\frac{x}{2}\right)^\alpha\left[1+O(x^2)\right], \qquad x\to 0.$$

H. Frequency Ramp Constraints

For a frequency ramp signal starting at nominal frequency, the input phasor within the frequency ramp time interval is $\mathcal{X}[n]=a_s e^{j\phi_s}e^{j\gamma n^2}$, $n=0,\dots,N_f-1$, where $\gamma=\pi R_f T^2$, being R_f the ramp rate, and N_f the sample length of the frequency ramp. We are interested in the estimations only within the exclusion interval limits, as defined on the IEEE Std., that is, for $n=n_1,\dots,n_2$, where n_1 is the first sample index after the initial exclusion interval and n_2 is the last sample index before the final exclusion interval. In this range, the filter bank outputs are as follows: $\widehat{\mathcal{X}}[n]=a_s e^{j\phi_s}e^{j\gamma n^2}\mathbf{b}_0^H[n]\mathbf{a}_0$, $\widehat{\mathcal{X}'}[n]=a_s e^{j\phi_s}e^{j\gamma n^2}\mathbf{b}_1^H[n]\mathbf{a}_1$, $\widehat{\mathcal{X}''}[n]=a_s e^{j\phi_s}e^{j\gamma n^2}\mathbf{b}_2^H[n]\mathbf{a}_2$,where $(\mathbf{b}_0^H[n])_{k_0}=\cos(2\gamma nk_0)e^{j\gamma k_0^2}$, $(\mathbf{b}_1^H[n])_{k_1}=j\sin(2\gamma nk_1)e^{j\gamma k_1^2}$, and $(\mathbf{b}_2^H[n])_{k_2}=\cos(2\gamma nk_2)e^{j\gamma k_2^2}$, with $k_0,k_2=0,\dots,R$ and $k_1=1,\dots,R$. Therefore, using the squared TVE, we obtain the following constraint:

$$\mathbf{a}_0^T\boldsymbol{P}_{00}[n]\mathbf{a}_0+\mathbf{q}_0^T[n]\mathbf{a}_0+1\le\text{TVE}^2_{\text{FR}}, \qquad n=n_1,\dots,n_2,$$

where $\boldsymbol{P}_{00}[n]=\mathbf{b}_0[n]\mathbf{b}_0^H[n]$ and $\mathbf{q}_0[n]=-2\,\text{Re}\{\mathbf{b}_0[n]\}$. In [18], the following semi-infinite approximation was proposed:

$$\mathbf{a}_0^T\boldsymbol{P}_{00}(\theta_0)\mathbf{a}_0+\mathbf{q}_0^T(\theta_0)\mathbf{a}_0+1-\text{TVE}^2_{\text{FR}}\le 0, \quad \theta_0\in[\theta_{\min},\theta_{\max}],$$

where $\theta_{\min}=\gamma n_1$, $\theta_{\max}=\gamma n_2$, and $\boldsymbol{P}_{00}(\theta_0)$, $\mathbf{q}_0(\theta_0)$ are obtained, respectively, from $\boldsymbol{P}_{00}[n]$ and $\mathbf{q}_0[n]$ by replacing γn by θ_0. Using the same approximation as for the TVE, we obtain the following FE and RFE constraints:

$$\left|\frac{\mathbf{a}_0^{*T}\boldsymbol{P}^I_{01}(\theta_1)\mathbf{a}_1}{\mathbf{a}_0^{*T}\boldsymbol{P}_{00}(\theta_1)\mathbf{a}_0^*}-\frac{2\theta_1}{T}\right|\le 2\pi\text{FE}_{\text{FR}}, \qquad \theta_1\in[\theta_{\min},\theta_{\max}],$$
$$\left|\frac{\mathbf{a}_0^{*T}\boldsymbol{P}^I_{02}(\theta_2)\mathbf{a}_2}{\mathbf{a}_0^{*T}\boldsymbol{P}_{00}(\theta_2)\mathbf{a}_0^*}-2\frac{\mathbf{a}_0^{*T}\boldsymbol{P}^R_{01}(\theta_2)\}\mathbf{a}_1^*}{\mathbf{a}_0^{*T}\boldsymbol{P}_{00}(\theta_2)\mathbf{a}_0^*}\frac{\mathbf{a}_0^{*T}\boldsymbol{P}^I_{01}(\theta_2)\mathbf{a}_1^*}{\mathbf{a}_0^{*T}\boldsymbol{P}_{00}(\theta_2)\mathbf{a}_0^*}-2\pi R_f\right|\le 2\pi\text{RFE}_{\text{FR}}, \qquad \theta_2\in[\theta_{\min},\theta_{\max}],$$

where $\boldsymbol{P}_{kl}(\theta_p)$ is obtained by replacing γn by θ_p in $\boldsymbol{P}_{kl}[n]=\mathbf{b}_k[n]\mathbf{b}_l^H[n]$, $\boldsymbol{P}^R_{kl}(\theta_p)=\text{Re}\{\boldsymbol{P}_{kl}(\theta_p)\}$, and $\boldsymbol{P}^I_{kl}(\theta_p)=\text{Im}\{\boldsymbol{P}_{kl}(\theta_p)\}$.

I. Amplitude and Phase Steps Constraints

The signal phasor for an amplitude step can be written as $\mathcal{X}[n]=a_s(1+\Delta a u[n])e^{j\phi_s}$, where $u[n]$ is the unit step signal and Δa is the amplitude step size. For the sake of simplicity, we present only the constraints for the case $\Delta a>0$, but the case $\Delta a<0$ is treated similarly. Note that amplitude overshoot (AO) can then be characterized as follows:

$$\text{AO}=\max_{n=0,\dots,R}\frac{|\widehat{\mathcal{X}}[n]|-|\mathcal{X}[n]|}{|\mathcal{X}[n]|}=\max_{n=0,\dots,R}\frac{(A_0(0)+\Delta a s_0[n])-(1+\Delta a)}{1+\Delta a},$$

where $A_0(0)=\mathbf{g}_0^T(0)\mathbf{a}_0$ and $s_0[n]=\mathbf{u}_0^T[n]\mathbf{a}_0$, with $(\mathbf{u}_0[n])_{k_0}=\frac{u[n+k_0]+u[n-k_0]}{2}$ for $k_0=0,\dots,R$. Thus, the constraint $\text{AO}\le\text{AO}_{\max}$ can be readily expressed as $R+1$

linear ordinary constraints on $\mathbf{a}_0$. Now, we obtain the response time constraints explicitly. Consider first the TVE:

$$\text{TVE}[n] = \frac{|(A_0(0) + \Delta a s_0[n]) - (1 + \Delta a u[n])|}{|1 + \Delta a u[n]|}.$$

Let $t_{r,\text{TVE}}$ be the desired value for the TVE response time and $n_{r,\text{TVE}} = \lfloor t_{r,\text{TVE}}/2T \rfloor$. The quantities $(t_{r,\text{FE}}, n_{r,\text{FE}})$, and $(t_{r,\text{RFE}}, n_{r,\text{RFE}})$ are defined analogously. Then, the TVE response time constraint can be formulated as[5] $\text{TVE}[n] \leq \text{TVE}_{\text{STA}}^{\text{STD}}$ for $n = -R, \ldots, -n_{r,\text{TVE}}, n_{r,\text{TVE}}, \ldots, R$, which translates to $4(R - n_{r,\text{TVE}} + 1)$ ordinary linear constraints on $\mathbf{a}_0$. Note that both $\widehat{\omega}[n]$ and $\widehat{\alpha}[n]$ are identically zero for amplitude steps, so that no additional constraints are required.

For a phase step, the signal phasor can be written as $\mathcal{X}[n] = a_s e^{j(\phi_s + \Delta\phi u[n])}$, where $\Delta\phi$ is the phase step size. Then, we obtain the following expressions for the FB outputs: $\widehat{\mathcal{X}}[n] = a_s e^{j\phi_s} \mathbf{v}_0^H[n]\mathbf{a}_0$, $\widehat{\mathcal{X}'}[n] = a_s e^{j\phi_s} \mathbf{v}_1^H[n]\mathbf{a}_1$, $\widehat{\mathcal{X}''}[n] = a_s e^{j\phi_s} \mathbf{v}_2^H[n]\mathbf{a}_2$, where $(\mathbf{v}_0^H[n])_{k_0} = \frac{e^{j\Delta\phi u[n+k]} + e^{j\Delta\phi u[n-k]}}{2}$, $(\mathbf{v}_1^H[n])_{k_1} = \frac{e^{j\Delta\phi u[n+k]} - e^{j\Delta\phi u[n-k]}}{2}$, $(\mathbf{v}_2^H[n])_{k_2} = \frac{e^{j\Delta\phi u[n+k]} + e^{j\Delta\phi u[n-k]}}{2}$, $k_0, k_2 = 0, \ldots, R$, $k_1 = 1, \ldots, R$. Let us also define the following matrices: $\boldsymbol{P}_{kl}[n] = \mathbf{v}_k[n]\mathbf{v}_l^H[n]$, $\boldsymbol{P}_{kl}^R[n] = \text{Re}(\boldsymbol{P}_{kl}[n])$, and $\boldsymbol{P}_{kl}^I[n] = \text{Im}(\boldsymbol{P}_{kl}[n])$, $k, l = 0, 1, 2$, which are required in what follows. Again, we consider only the case $\Delta\phi > 0$ for simplicity of presentation. Then, phase overshoot (PO) can be characterized as:

$$\text{PO} = \max_{n=0,\ldots,R} \frac{\angle\widehat{\mathcal{X}}[n] - \angle\mathcal{X}[n]}{\Delta\phi} = \max_{n=0,\ldots,R} \frac{\angle\mathbf{v}_0^H[n]\mathbf{a}_0 - \Delta\phi}{\Delta\phi}.$$

Unfortunately, the constraint $\text{PO} \leq \text{PO}_{\max}$ leads to several non-convex constraints. However, noting that $\angle\mathbf{v}_0^H[n]\mathbf{a}_0$ should oscillate in a small neighborhood around $\Delta\phi$ after the step, we can relax the constraint by

$$\text{Im}\{\mathbf{v}_0^H[n]\}\mathbf{a}_0 \leq \tan[\Delta\phi(1 + \text{PO}_{\max})]\,\text{Re}\{\mathbf{v}_0^H[n]\}\mathbf{a}_0,$$

for $n = 0, \ldots, R$, which are $R + 1$ ordinary linear constraints on $\mathbf{a}_0$. To obtain the response time constraints we proceed as with the amplitude step test. In this case, the TVE response time constraint can be written as follows:

$$\text{TVE}^2[n] = \mathbf{a}_0^T \boldsymbol{P}_{00}[n]\mathbf{a}_0 + \mathbf{q}_0^T[n]\mathbf{a}_0 + 1 \leq (\text{TVE}_{\text{STA}}^{\text{STD}})^2,$$

where $\mathbf{q}_0^T[n] = -2\,\text{Re}\{e^{-j\Delta\phi u[n]}\mathbf{v}_0^H[n]\}$, for $n = -R, \ldots, -n_{r,\text{TVE}}, n_{r,\text{TVE}}, \ldots, R$. Similarly, the FE response time constraint is:

$$\text{FE}[n] = \frac{1}{2\pi}\left|\frac{\mathbf{a}_0^{*T}\boldsymbol{P}_{01}^I[n]\mathbf{a}_1}{\mathbf{a}_0^{*T}\boldsymbol{P}_{00}[n]\mathbf{a}_0^*}\right| \leq \text{FE}_{\text{STA}}^{\text{STD}},$$

for $n = -R, \ldots, -n_{r,\text{FE}}, n_{r,\text{FE}}, \ldots, R$. Finally, the ROCOF estimate is:

$$\widehat{\alpha}[n] = \frac{\mathbf{a}_0^{*T}\boldsymbol{P}_{02}^I[n]\mathbf{a}_2}{\mathbf{a}_0^{*T}\boldsymbol{P}_{00}[n]\mathbf{a}_0^*} - 2\frac{\mathbf{a}_0^{*T}\boldsymbol{P}_{01}^R[n]\mathbf{a}_1^*}{\mathbf{a}_0^{*T}\boldsymbol{P}_{00}[n]\mathbf{a}_0^*}\frac{\mathbf{a}_0^{*T}\boldsymbol{P}_{01}^I[n]\mathbf{a}_1^*}{\mathbf{a}_0^{*T}\boldsymbol{P}_{00}[n]\mathbf{a}_0^*}.$$

Then, the RFE response time constraint can be written as follows:

$$\text{RFE}[n] = \frac{1}{2\pi}|\widehat{\alpha}[n]| \leq \text{RFE}_{\text{STA}}^{\text{STD}},$$

for $n = -R, \ldots, -n_{r,\text{RFE}}, n_{r,\text{RFE}}, \ldots, R$.

J. Other Constraints

In more general terms, let $\mathcal{X}_{\boldsymbol{\theta}}[n]$, $\mathcal{X}'_{\boldsymbol{\theta}}[n]$, and $\mathcal{X}''_{\boldsymbol{\theta}}[n]$ be the input phasor and its derivatives associated with a particular waveform parameterized by $\boldsymbol{\theta} \in \Theta$. Suppose also that we are interested in the errors on the index set $\mathcal{N} \subseteq \mathbb{Z}$. Note that $\widehat{\mathcal{X}}[n] = \mathbf{b}_{\boldsymbol{\theta},0}^H[n]\mathbf{a}_0$, $\widehat{\mathcal{X}'}[n] = \mathbf{b}_{\boldsymbol{\theta},1}^H[n]\mathbf{a}_1$, and $\widehat{\mathcal{X}''}[n] = \mathbf{b}_{\boldsymbol{\theta},2}^H[n]\mathbf{a}_2$ for some $\mathbf{b}_{\boldsymbol{\theta},0}[n], \mathbf{b}_{\boldsymbol{\theta},2}[n] \in \mathbb{C}^{R+1}$ and $\mathbf{b}_{\boldsymbol{\theta},1}[n] \in \mathbb{C}^R$. Consider the TVE, the FE and the RFE: $\text{TVE}_{\boldsymbol{\theta}}[n]$, $\text{FE}_{\boldsymbol{\theta}}[n]$, and $\text{RFE}_{\boldsymbol{\theta}}[n]$, where $(n, \boldsymbol{\theta}) \in \mathcal{N} \times \Theta$. It is clear that the constraints $\text{TVE}_{\boldsymbol{\theta}}[n] \leq \varepsilon_{\text{TVE}}$, $\text{FE}_{\boldsymbol{\theta}}[n] \leq \varepsilon_{\text{FE}}$, and $\text{RFE}_{\boldsymbol{\theta}}[n] \leq \varepsilon_{\text{RFE}}$, for all $(n, \boldsymbol{\theta}) \in \mathcal{N} \times \Theta$ and for given parameters ε_{TVE}, ε_{FE}, $\varepsilon_{\text{RFE}} > 0$, are convex semi-infinite constraints. The challenge, of course, is to simplify

$$\widehat{\omega}(\nu_s, \nu_i, \theta) = \frac{A_0^*(\nu_s)A_1(\nu_s) + \eta^2 A_0^*(\nu_i)A_1(\nu_i) + \eta[A_0^*(\nu_s)A_1(\nu_i) + A_0^*(\nu_i)A_1(\nu_s)]\cos(\theta)}{A_0^{*2}(\nu_s) + \eta^2 A_0^{*2}(\nu_i) + 2\eta A_0^*(\nu_s)A_0^*(\nu_i)\cos(\theta)}. \tag{3}$$

$$\widehat{\alpha}(\nu_s, \nu_i, \theta) = \frac{[A_0^*(\nu_s)A_2(\nu_i) - A_0^*(\nu_i)A_2(\nu_s)]\eta\sin(\theta)}{A_0^{*2}(\nu_s) + A_0^{*2}(\nu_i)\eta^2 + 2A_0^*(\nu_s)A_0^*(\nu_i)\eta\cos(\theta)} - 2\frac{[A_0^*(\nu_i)A_1^*(\nu_s) - A_0^*(\nu_s)A_1^*(\nu_i)]\eta\sin(\theta)}{A_0^{*2}(\nu_s) + A_0^{*2}(\nu_i)\eta^2 + 2A_0^*(\nu_s)A_0^*(\nu_i)\eta\cos(\theta)} \times \frac{A_0^*(\nu_s)A_1^*(\nu_s) + A_0^*(\nu_i)A_1^*(\nu_i)\eta^2 + A_0^*(\nu_s)A_1^*(\nu_i)\eta\cos(\theta) + A_0^*(\nu_i)A_1^*(\nu_s)\eta\cos(\theta)}{A_0^{*2}(\nu_s) + A_0^{*2}(\nu_i)\eta^2 + 2A_0^*(\nu_s)A_0^*(\nu_i)\eta\cos(\theta)}. \tag{5}$$

$$\begin{aligned}
\widehat{\mathcal{X}_R}[n] &= A_0(0)J_0(k_\phi) + 2\sum_{k=1}^{\infty}(-1)^k A_0(2k\nu_m)J_{2k}(k_\phi)\cos(2k\theta_m), & \widehat{\mathcal{X}_I}[n] &= 2\sum_{k=0}^{\infty}(-1)^k A_0((2k+1)\nu_m)J_{2k+1}(k_\phi)\cos[(2k+1)\theta_m], \\
\widehat{\mathcal{X}'_R}[n] &= -2\sum_{k=1}^{\infty}(-1)^k A_1(2k\nu_m)J_{2k}(k_\phi)\sin(2k\theta_m), & \widehat{\mathcal{X}'_I}[n] &= -2\sum_{k=0}^{\infty}(-1)^k A_1((2k+1)\nu_m)J_{2k+1}(k_\phi)\sin[(2k+1)\theta_m], \\
\widehat{\mathcal{X}''_R}[n] &= A_2(0)J_0(k_\phi) + 2\sum_{k=1}^{\infty}(-1)^k J_{2k}(k_\phi)A_2(2k\nu_m)\cos(2k\theta_m), & \widehat{\mathcal{X}''_I}[n] &= 2\sum_{k=0}^{\infty}(-1)^k J_{2k+1}(k_\phi)A_2((2k+1)\nu_m)\cos[(2k+1)\theta_m].
\end{aligned} \tag{6}$$

[5] We will use the superscript STD to denote the performance limits defined in the IEEE Std. [1], [2].

the constraints as much as possible by exploiting the structure of $\text{TVE}_{\boldsymbol{\theta}}[n]$, $\text{FE}_{\boldsymbol{\theta}}[n]$, and $\text{RFE}_{\boldsymbol{\theta}}[n]$. This general approach was demonstrated extensively in this section.

III. Numerical Results

In this section, we present several numerical results which provide very useful information for the synchrophasor estimation problem and also illustrate the advantages of the optimization approach. Firstly, we study the achievable uniform performance of the linear-phase filter bank structure, which is a simple and convenient worst-case characterization of this class of algorithms. Secondly, a P class PMU design example is presented and an interesting comparison is made with the TF filters [12]. In all cases, we consider a reporting rate of $F_s = 50$ fps, a nominal frequency of $f_0 = 50$ Hz and a sampling period of $T = (20 \times f_0)^{-1} = 1$ ms. We have used a relatively low sampling rate for computational efficiency and since it was observed that achievable performance is practically independent of T. The constraint parameters were taken from the current IEEE Std. version.

A. Uniform Feasibility Limits

We let $\mathcal{P}_i(\rho_i)$, for $i = 0, 1, 2$, be the optimization problem associated with the design of the i-th filter obtained by setting the free design parameters to the corresponding IEEE Std. constraint limits scaled by the common factor[6] ρ_i. We also define ρ_i^* as the infimum of the set of all ρ_i such that $\mathcal{P}_i(\rho_i)$ is feasible. Thus, the number ρ_i^* represents a uniform feasibility limit for the i-th filter design problem. It is important to realize that ρ_i^* is determined solely by the most severe constraints and is independent of the choice of the cost functions. We use this partial characterization for its ease of presentation. Clearly, ρ_i^* is a function of K, the cycle length of the filter[7]. Note that $\rho_i^* > 1$ indicates that a IEEE Std. compliant design is not feasible for that particular value of K. The range of values of K considered is such that the maximum value of K gives a full latency system, that is, a system with delay equal to the maximum PMU reporting latency. In Tables I and II, we present the values of ρ_i^* for different values of K for P and M class PMUs, respectively. These results provide the following important insights:

1) It is observed that a feasible P class filter A_0 can be obtained with a simple one-cycle filter and provide a uniform performance of $\rho_0^* = 0.36$, that is, at most 36% of the IEEE Std. limits. For the M class PMU, instead, a four-cycle filter is required for feasibility and $\rho_0^* = 0.53$. These results show that it is possible to obtain accurate phasor estimates with low latency. Thus, the M class specifications are considerably more stringent than the P class ones. This is primarily due to the more strict interference rejection requirements.

[6]For example, $\mathcal{P}_0(\rho_0)$ represents the problem of minimizing f_0 subject to all the constraints on a_0 from Sections II-E to II-I, with TVE_{STA} replaced by $\rho_0 \text{TVE}_{\text{STA}}^{\text{STD}}$, and the other parameters are defined analogously.

[7]Of course, it is not strictly necessary to design the filters with a length equal to an integer number of cycles, so K needs not to be an integer. However, both for convenience of presentation and since it is customary in the literature, we will consider only integer values for K.

TABLE I
Uniform Feasibility Limits for P class PMU

K	ρ_0^*	ρ_1^*	ρ_2^*
1	0.36	18.9	2.46
2	0.36	1.13	1.92
3	0.36	0.57	0.50
4	0.33	0.55	0.50

2) The first differentiator filter A_1 requires a three-cycle filter for the P class PMU which yields $\rho_1^* = 0.57$, while no feasible A_1 filter was found for the M class PMU specifications. Previous conjectures claim that most of the available algorithms use windows that are too short to be compliant with the interharmonic rejection constraint [8], [14], particularly for M class specifications. The result we have found is very important since it shows that[8], for a linear-phase differentiator filter bank, there is no filter such that all the M class constraints are achieved. Concretely, this happens because the FE constraint for out-of-band interference is too stringent considering the required bandwidth of the A_1 filter. To address this problem, a more sophisticated scheme could be used in order to relax the design constraints. For example, an adaptive interference canceler such as the one proposed in [11] based on the IpDFT could be used to eliminate or at least significantly attenuate the interharmonic components with little influence on the fundamental signal phasor. This would, in turn, give much more freedom for the design of the A_1 filter so that other performance aspects may also be enhanced. Of course, the study of this or other extensions requires further research.
3) The second differentiator filter A_2 also requires a three-cycle filter for the P class PMU, yielding $\rho_2^* = 0.50$. This shows that the RFE constraints of the IEEE Std. are slightly less stringent than the FE ones. Since the RFE limits in the presence of harmonics and interharmonics have been suspended for the M class PMU [2] (the practical implications of this are discussed, for example, in [14]), the results of the feasibility analysis for the A_2 filter show that ρ_2^* is very small. This is reasonable since the elimination of these limits removes the signal distortion-interference rejection trade-off of the filter design problem.
4) Clearly, ρ_i^* are non-increasing functions of K, that is, longer filters always provide at least the same achievable performance than shorter ones[9]. However, it is observed that a saturation phenomenon occurs in all cases, showing that ρ_i^* can not be made arbitrarily small by increasing K. Thus, there is a "corner" filter length for each problem, in the sense that longer filters provide virtually no gain in terms of performance. This is a very interesting result with important practical implications.

[8]Of course that this holds up to the numerical accuracy of the solver.

[9]A strange exception occurs for ρ_2^* in the M class PMU, but this is irrelevant because of their magnitude. Moreover, ρ_1^* for the M class PMU is not strictly non-increasing, which is probably due to small numerical errors of the solver.

TABLE II
UNIFORM FEASIBILITY LIMITS FOR M CLASS PMU

K	ρ_0^*	ρ_1^*	ρ_2^*	K	ρ_0^*	ρ_1^*	ρ_2^*
1	4.36	166	0.03	8	0.49	1.18	0.11
2	3.03	48.3	0.05	9	0.49	1.18	0.10
3	1.63	20.1	0.09	10	0.49	1.18	0.08
4	0.53	18.2	0.04	11	0.49	1.18	0.10
5	0.50	6.41	0.06	12	0.49	1.18	0.10
6	0.49	2.31	0.09	13	0.48	1.20	0.05
7	0.49	1.27	0.10	14	0.48	1.20	0.05

At this point, it is interesting to compare the performance limits with results obtained with a much more complex system, such as the modular system described in [22], which is based on a demodulation stage, a prefiltering stage, a phase-locked loop, and a compensation stage. An interesting difference is that the aforementioned method does not use a fixed window at each reporting time but it is based on a recursive sample-by-sample approach. The system is fully compliant with the IEEE Std. as can be seen from the results reported in [22], but its uniform performance may be poorer than that of the filter bank. For example, for the P class PMU, the phase overshoot is 4.302%, the FE response time is 89 ms and the RFE response time is 100 ms. This means that for that system $\rho_0 \geq 0.86$, $\rho_1 \geq 0.99$, and $\rho_2 \geq 0.83$. Thus, the P class system designed with the approach presented in this paper can provide not only a better uniform performance but it does so with a much smaller real-time computational burden. The point here is that using a more complex method does not necessarily mean that the obtained performance will be better. Here, the optimization approach outperforms the more sophisticated system by using optimally all its degrees of freedom. This can never be guaranteed with a trial and error design approach.

B. Design Examples

We consider a P class example and compare the CSIP filters against the well-known Taylor-Fourier filters [6], [7]. Motivated by the results of Section III-A, we will use four-cycle length filters. For the objective functions, we set $\lambda_i = 0$, so that we seek to minimize the stopband energy of the filters A_i. The constraints are the ones found in the IEEE Std., so that $\rho_i = 1$, and we have also added the linear constraints $A_0(0) = 1$ and $A_2(0) = 0$, which ensures that the system operates with no error at nominal frequency. Magnitude and impulse responses of the CSIP filters[10] are presented in Fig. 3, showing also the TF filters responses, which are based on a third-order Taylor approximation and use a Kaiser window (with parameter $\alpha = 8$) as in [7]. It is interesting to observe that the TF filters, with this particular window choice, yield greater stopband attenuation at the expense of an excessive bandwidth. This is actually detrimental to the PMU interference rejection capability. Of course, as the optimization problem formulation shows, there are also other performance differences which are not so readily inferred from the magnitude/impulse responses. In the following, we perform several performance tests to analyze the differences between these systems and validate the proposed CSIP design method.

1) Stationary Tests: Firstly, both systems are tested with a sinusoidal input signal whose frequency f_s is swept in the off-nominal range defined in the IEEE Std. Results are shown in Fig. 2 for TVE and FE. The RFE results are not shown since for both systems RFE $= 0$ (up to numerical errors) due to the linear-phase of the filters (see Section II-E). The TF system shows a better behavior in this case due to its maximal flatness property [7], but the CSIP system satisfies the IEEE Std. limits as prescribed. If desired, it is straightforward to improve a particular performance metric. For example, since the FE constraint is active, in practice it would reasonable to reduce the parameter FE_{STA} and redesign the system. Interestingly, one could also include the maximal flatness condition in the CSIP design problem, since the constraints of the form $A_i^{(k)}(0) = c_{ik}$ are linear in the filters coefficients.

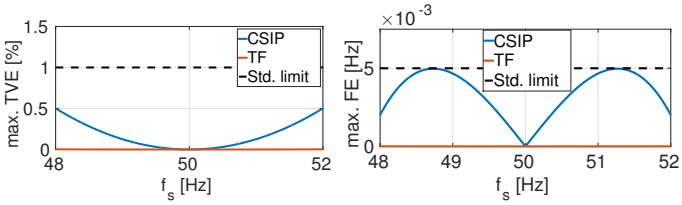

(a) TVE (b) FE

Fig. 2. Maximum TVE and FE for off-nominal frequencies.

Secondly, harmonic interference rejection is evaluated at a total harmonic distortion (THD) level of 1% for the first ten harmonics individually. Worst-case TVE, FE, and RFE for both systems occur with the first harmonic and are given in Table III. In this case, the CSIP clearly outperforms the TF system and the latter is not compliant with the FE and RFE requirements of the IEEE Std. This occurs due to the excessive bandwidth of the TF filters, as was noticed before.

TABLE III
HARMONIC DISTORTION RESULTS

	CSIP	TF	
Metric	Result	Result	Std. limit
max. TVE [%]	0.0020	0.0356	1
max. FE [Hz]	2.9672×10^{-5}	0.0248	0.0050
max. RFE [Hz/s]	0.0105	1.0710	0.4000

2) Dynamic Tests:

a) Amplitude and Phase Modulation: The maximum TVE, FE, and RFE for amplitude and phase modulation (AM and PM, respectively) tests as a function of the modulation frequency f_m are shown in Fig. 4. Note that the worst-case errors occur for the maximum value of f_m. The maximum FE and RFE results are not shown for the amplitude modulation test since they are zero (up to numerical errors) as explained in Section II-G. We observe again that the TF results are better

[10]The solver was run on a desktop computer with an Intel Core i7-4790 processor and the time required to obtain the CSIP filters was in the order of a few seconds. Concretely, for a typical run, the solver time for the filters A_0, A_1 and A_2, was 4.344 s, 21.061 s, and 30.801 s, respectively. For the filters initialization, we used traditional equiripple filters with the desired passband and stopband frequencies.

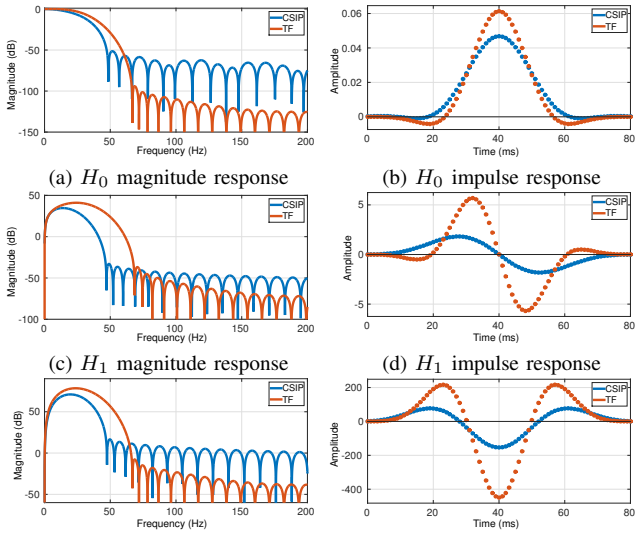

(a) H_0 magnitude response (b) H_0 impulse response

(c) H_1 magnitude response (d) H_1 impulse response

(e) H_2 magnitude response (f) H_2 impulse response

Fig. 3. Comparison between TF and CSIP filters (with $\lambda_i = 0$ and $\rho_i = 1$) for P class PMU.

TABLE IV
MODULATION TEST RESULTS

	Metric	CSIP	TF	Std. limit
AM	max. TVE [%]	0.0558	2.7×10^{-4}	3
	max. FE [Hz]	~ 0	~ 0	0.06
	max. RFE [Hz/s]	~ 0	~ 0	2.3
PM	max. TVE [%]	0.0502	2.5049e-04	3
	max. FE [Hz]	8.1×10^{-4}	4.4×10^{-6}	0.06
	max. RFE [Hz/s]	1.0195	0.0169	2.3

than those of the CSIP due to its flatness property. However, both systems perform well below the IEEE Std. limits as can be seen in Table IV.

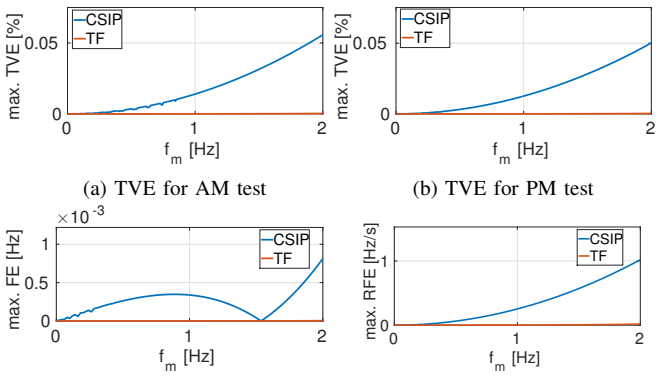

(a) TVE for AM test (b) TVE for PM test

(c) FE for PM test (d) RFE for PM test

Fig. 4. Modulation test results.

b) Frequency Ramp: In Fig. 5 we can see the performance for both systems when a frequency ramp between 48 and 52 Hz is performed at a ramp rate of 1 Hz/s starting at $t = 1$ s. Note that, once again, the flatness property of the TF filters translates to very good results. The CSIP system works as prescribed, in the sense that it is compliant with the IEEE Std. limits that were imposed in its design. Again, since the RFE constraint is active, for a practical design one could reduce the parameter RFE_{FR} in order to obtain a suitable performance margin.

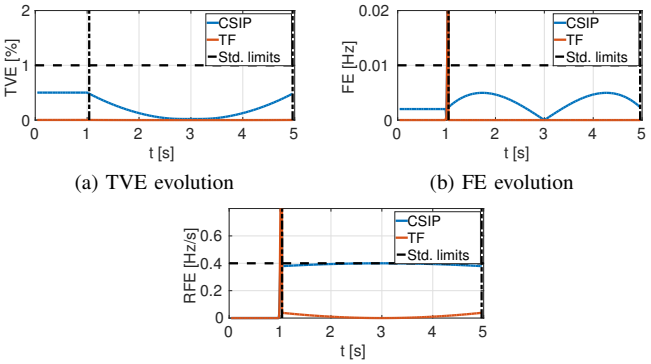

(a) TVE evolution (b) FE evolution

(c) RFE evolution

Fig. 5. Frequency ramp test.

c) Amplitude and Phase Step Tests: Results for each of the step tests described in the IEEE Std. are shown in Table V. Note that the TF system provides fast responses, which is expected due to its bigger bandwidth. On the other hand, its overshoot is much greater than that of the CSIP, which is due to the limitations of its parametric polynomial model, as mentioned in Section I. To illustrate these results, the phase step responses of both systems are shown in Fig. 6.

TABLE V
STEP TEST RESULTS

	CSIP			TF		
Metric	Amp.	Phase	Std. limit	Amp.	Phase	Std. limit
Over. [%]	0.2264	0.2252	5	3.9526	3.9302	5
$t_{r,\text{TVE}}$ [s]	0.0210	0.0270	0.04	0.016	0.0190	0.04
$t_{r,\text{FE}}$ [s]	0	0.0690	0.09	0	0.0670	0.09
$t_{r,\text{RFE}}$ [s]	0	0.0730	0.12	0	0.0670	0.12

3) Discussion: In summary, for this design example, the TF system showed better performance in dynamic and off-nominal conditions due to both its bigger bandwidth and flatness property. However, this performance enhancement came at the expense of a poor harmonic rejection capability. Moreover, it inevitably leads to a time-consuming trial and error process if one wants to improve the TF system performance. As mentioned in Section I, that approach does not guarantee that a system fully compliant with the IEEE Std. will be found. Overall, the uniform performance of the CSIP system is better than that of the TF, since only the former is fully compliant with the IEEE Std. requirements. In fact, considering the harmonic distortion test, $\rho_1 > 1$ and $\rho_2 > 1$ for the TF system, while the step test results show that $\rho_0 \geq 0.79$. Interestingly, this is much greater than the feasibility limit of $\rho_0^* = 0.33$ presented in Table I, which indicates that the TF system performance is significantly worst than the ultimate achievable performance.

IV. CONCLUSIONS

In this paper, we have applied the powerful tool of convex semi-infinite optimization for the design of a filter bank for the dynamic phasor estimation problem. This extends the

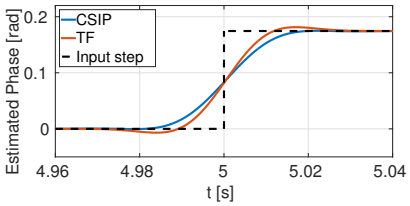

Fig. 6. Phase step response.

work [18] in a meaningful way by adding two differentiators which are required to obtain frequency and ROCOF estimates. We have treated in detail the positive-sequence estimation problem, but the approach is quite general and suitable for both three-phase and single-phase signals. It allows to pose the estimation problem in an explicit form (i.e., each performance constraint can be included), thus providing a complete control over the behavior of the system. An important consequence of this fact is that the method requires no trial and error, thus simplifying enormously the designer task. The main problem that is left to the designer is the decision of which factors should be prioritized, which is highly dependent on the particular application of the synchrophasor measurements.

We have also presented the uniform feasibility limits for the problem, a partial characterization of the filter bank which provides useful information with respect to what can be achieved with a given filter length. It is important to note that the results reveal not a limit of the filter design method but rather an intrinsic limit of the fixed-filtering filter bank structure. The results obtained here could be useful as guidelines for designers and, moreover, in future revisions or extensions of the IEEE Std. One particularly important algorithm which belongs to the same class as our method is given by the Taylor-Fourier filters, for which a comparison example has been given to show the benefits of our approach.

Finally, it is expected that the CSIP approach will be extremely useful for designing prototype filters to use in more sophisticated adaptive schemes if the required performance is beyond the feasibility limits of the rigid fixed-filtering approach. For example, an adaptation based on instantaneous frequency-tracking can relax the off-nominal frequency constraints, while online spectral analysis could help loosening up the tight distortion-filtering trade-off which is inescapable for any fixed-filtering based algorithm. As the feasibility limits show, these extensions may be required to achieve the FE interharmonic rejection constraint of the M class PMU. In any case, if these relaxations are well characterized (as they should), the approach can incorporate them beforehand to produce an enhancement in system performance. It should be mentioned that we are currently working on this interesting problem.

REFERENCES

[1] *IEEE Standard for Synchrophasor Measurements for Power Systems*, IEEE Std. C37.118.1-2011 (Revision of IEEE Std C37.118-2005), Dec. 2011.

[2] *IEEE Standard for Synchrophasor Measurements for Power Systems – Amendment 1: Modification of Selected Performance Requirements*, IEEE Std. C37.118.1a-2014 (Amendment to IEEE Std C37.118.1-2011), Apr. 2014.

[3] A. Phadke and J. Thorp, *Synchronized Phasor Measurements and Their Applications*, ser. Power Electronics and Power Systems. Springer US, 2008.

[4] D. Macii, D. Petri, and A. Zorat, "Accuracy Analysis and Enhancement of DFT-Based Synchrophasor Estimators in Off-Nominal Conditions," *IEEE Trans. Instrum. Meas.*, vol. 61, no. 10, pp. 2653–2664, Oct. 2012.

[5] D. Belega and D. Petri, "Accuracy Analysis of the Multicycle Synchrophasor Estimator Provided by the Interpolated DFT Algorithm," *IEEE Trans. Instrum. Meas.*, vol. 62, no. 5, pp. 942–953, May 2013.

[6] J. A. de la O Serna, "Dynamic Phasor Estimates for Power System Oscillations," *IEEE Trans. Instrum. Meas.*, vol. 56, no. 5, pp. 1648–1657, Oct. 2007.

[7] M. A. Platas-Garza and J. A. de la O Serna, "Dynamic Phasor and Frequency Estimates Through Maximally Flat Differentiators," *IEEE Transactions on Instrumentation and Measurement*, vol. 59, no. 7, pp. 1803–1811, July 2010.

[8] D. Petri, D. Fontanelli, and D. Macii, "A frequency-domain algorithm for dynamic synchrophasor and frequency estimation," *IEEE Trans. Instrum. Meas.*, vol. 63, no. 10, pp. 2330–2340, Oct. 2014.

[9] G. Barchi, D. Macii, and D. Petri, "Synchrophasor estimators accuracy: A comparative analysis," *IEEE Trans. Instrum. Meas.*, vol. 62, no. 5, pp. 963–973, May 2013.

[10] G. Barchi, D. Macii, D. Belega, and D. Petri, "Performance of synchrophasor estimators in transient conditions: A comparative analysis," *IEEE Trans. Instrum. Meas.*, vol. 62, no. 9, pp. 2410–2418, Sept 2013.

[11] D. Belega, D. Fontanelli, and D. Petri, "Dynamic phasor and frequency measurements by an improved taylor weighted least squares algorithm," *IEEE Transactions on Instrumentation and Measurement*, vol. 64, no. 8, pp. 2165–2178, Aug 2015.

[12] M. A. Platas-Garza and J. A. de la O Serna, "Dynamic harmonic analysis through taylor-fourier transform," *IEEE Transactions on Instrumentation and Measurement*, vol. 60, no. 3, pp. 804–813, March 2011.

[13] D. Macii, G. Barchi, and D. Petri, "Design criteria of digital filters for synchrophasor estimation," in *2013 IEEE International Instrumentation and Measurement Technology Conference (I2MTC)*, May 2013, pp. 1579–1584.

[14] A. J. Roscoe, B. Dickerson, and K. E. Martin, "Filter design masks for c37.118.1a-compliant frequency-tracking and fixed-filter m-class phasor measurement units," *IEEE Trans. Instrum. Meas.*, vol. 64, no. 8, pp. 2096–2107, Aug 2015.

[15] A. W. Potchinkov, "Design of optimal linear phase fir filters by a semi-infinite programming technique," *Signal Processing*, vol. 58, no. 2, pp. 165–180, 1997.

[16] R. Reemtsen and J. Rückmann, *Semi-Infinite Programming*, ser. Nonconvex Optimization and Its Applications. Springer US, 1998.

[17] C. Y. F. Ho, B. W. K. Ling, Y. Q. Liu, P. K. S. Tam, and K. L. Teo, "Optimum design of discrete-time differentiators via semi-infinite programming approach," *IEEE Transactions on Instrumentation and Measurement*, vol. 57, no. 10, pp. 2226–2230, Oct 2008.

[18] F. Messina, P. Marchi, L. Rey Vega, and C. G. Galarza, "Design of Synchrophasor Estimation Systems with Convex Semi-Infinite Programming," in *Electrical Power and Energy Conference (EPEC)*, Ottawa, Canada, Oct. 2016.

[19] MATLAB, *Optimization Toolbox*. Natick, Massachusetts: The MathWorks Inc., 2016.

[20] "Semi-infinite programming solvers: CSIP and NSIPS," http://www.norg.uminho.pt/aivaz/software.html.

[21] M. Abramowitz and I. Stegun, *Handbook of Mathematical Functions: With Formulas, Graphs, and Mathematical Tables*, ser. Applied mathematics series. Dover Publications, 1964. [Online]. Available: https://books.google.com.ar/books?id=MtU8uP7XMvoC

[22] F. Messina, P. Marchi, L. R. Vega, C. G. Galarza, and H. Laiz, "A novel modular positive-sequence synchrophasor estimation algorithm for pmus," *IEEE Transactions on Instrumentation and Measurement*, vol. PP, no. 99, pp. 1–12, 2017.